

Carsten Lukas
Horst K. Hahn
Barbara Bellenberg
Kerstin Hellwig
Christoph Globas
Sebastian K. Schimrigk
Odo Köster
Ludger Schöls

Spinal cord atrophy in spinocerebellar ataxia type 3 and 6

Impact on clinical disability

Received: 31 May 2007
Accepted in revised form: 16 January 2008
Accepted: 13 February 2008
Published online: 5 June 2008

C. Globas, MD · L. Schöls, MD
Dept. of Neurology and Hertie-Institute for
Clinical Brain Research
University of Tübingen
Hoppe-Seyler-Str. 3
72076 Tübingen, Germany

C. Lukas, MD (✉) · O. Köster, MD
Dept. of Diagnostic and Interventional
Radiology and Nuclear Medicine
St. Josef Hospital
Ruhr University Bochum
Gudrunstr. 56
44791 Bochum, Germany
Tel.: +49-234/509-0
Fax: +49-234/509-3307
E-Mail:
Carsten.Lukas@ruhr-uni-bochum.de

H. K. Hahn, PhD
MeVis Research
Universitaetsallee 29
28359 Bremen, Germany

B. Bellenberg, PhD · K. Hellwig, MD ·
S. K. Schimrigk, MD
Dept. of Neurology
St. Josef Hospital
Ruhr University Bochum
Gudrunstr. 56
44791 Bochum, Germany

■ **Abstract** *Objective* To quantify spinal cord atrophy and its impact on clinical disability in spinocerebellar ataxia (SCA) type 3 and 6. *Methods* Atrophy of the upper spinal cord was assessed by high resolution T1-weighted MRI of patients with SCA3 (n = 14) and SCA6 (n = 10). Furthermore, two groups of age- and sex-matched healthy control subjects (n = 24,) corresponding to the two SCA groups, were studied. Images were post-processed by a semi-automated volumetry method combining a marker based segmentation and an automatic histogram method facilitating highly reliable quantification and morphometry of the upper cervical cord in vivo. *Results* We found a significant reduction of normalized mean cross-

sectional area of the spinal cord in SCA3 ($p < 0.0005$), whereas in SCA6 patients normalized mean cross-sectional area was in the normal range ($p = 0.379$). No correlation was found between spinal cord atrophy and disease duration as well as CAG repeat length in both subtypes. In SCA6 a negative dependency between clinical disability, as expressed by the International Cooperative Ataxia Rating Scale as a well established ataxia score, and the mean cross-sectional area was found ($p = 0.02$). A similar correlation was observed in SCA3 but did not reach statistical significance. *Conclusion* Our results quantify for the first time in vivo spinal cord atrophy as a non-cerebellar neurodegenerative process in SCA3. Our results suggest MR volumetry of the upper cervical cord as a marker of functional importance in SCA3 and SCA6.

■ **Key words** spinocerebellar ataxia type 3 and type 6 · spinal cord atrophy · MRI

Introduction

Spinocerebellar ataxia (SCA) comprises a clinically and genetically heterogeneous group of autosomal dominant disorders characterized by progressive ataxia due to cerebellar degeneration. Affection of additional parts of the central and peripheral nervous system occurs in

several but not all subtypes and is associated with reduced life expectancy [5]. Conventional magnetic resonance imaging (MRI) in SCA usually focuses on cerebellar and pontine atrophy. In SCA6 atrophy is mainly limited to the cerebellum [12, 15], whereas in SCA3 additional involvement of cerebral cortex, basal ganglia and the ponto-medullary systems is detected on MRI [6, 13, 17, 23].

So far, spinal cord atrophy has not systematically been studied in SCA3 and SCA6 on MRI. In Friedreich's ataxia, the most common autosomal recessive ataxia in Caucasians, atrophy of the spinal cord is the most prominent change on MRI and occurs mainly in the cervical spine [2, 9, 21, 22]. Histopathologically these changes in Friedreich's ataxia are due to degeneration of the posterior and lateral white matter tracts [2, 21]. In multiple sclerosis the spinal cord is commonly affected by the disease with MR studies revealing significant correlations between clinical disability and cervical cord atrophy. Its impact on functional impairment reveals an important biomarker of disease progression in multiple sclerosis [1, 10, 14].

To study the development of spinal cord atrophy in SCA and to assess its impact on disability we performed a quantitative volumetric study of the upper spinal cord volume in patients suffering from the most frequent subtypes of spinocerebellar ataxia in Germany, SCA3 and SCA6 [18].

Methods

Subjects

Fourteen subjects with a molecular diagnosis of SCA3 and ten subjects with genetically proven SCA6 were recruited from the ataxia outpatient clinic in Bochum. Disease onset was earlier in SCA3 (41 ± 5.1 years) than in the SCA6 group (59 ± 6.8 years). For comparison, two groups of age- and sex-matched healthy controls corresponding to both SCA subtypes with no history of neurological or psychiatric diseases were examined. Detailed description of the study groups is provided in Table 1. Disability in SCA was scored according to the International Cooperative Ataxia Rating Scale (ICARS) [20].

All subjects underwent a standardized MRI protocol and neurological examination. Pyramidal tract affection was presumed when spasticity, hyperreflexia or extensor plantar response (Babinski's sign) was present. Involvement of sensory afferent tracts was assumed when vibration sense ($< 6/8$), joint position sense, pinprick or temperature discrimination was impaired. The study protocol was approved by the local ethics committee. All individuals gave their written informed consent to MRI examinations and further use of anonymized data.

Neuroimaging and data analysis

All MRI examinations were performed on a 1.5 T scanner (Magnetom Symphony™, Siemens, Erlangen, Germany). A standard head coil was

used to acquire sagittal high resolution T1-weighted 3D MRI data (MPRAGE) covering the whole brain and upper cervical spinal cord. A Turbo FLASH 3D sequence with the following parameters was used in this study: TE (echo time): 3.93 ms, TR (repetition time): 1900 ms, TI (inversion time): 1100 ms, FA: 15°, NA: 1, resolution: 1 mm × 1 mm, 128 sagittal slices, slice thickness: 1.5 mm, scan time: 8 min 40 s. The subjects were positioned within the head coil using a standard procedure according to outer anatomical markers.

Post-processing of MR images

Images were post-processed by using a semi-automated volumetry method combining a marker based segmentation and an automatic histogram analysis [7]. Spinal cord volume was segmented and quantified within a section of 50 mm thickness starting at upper border of C2 rostrally (Fig. 1). To facilitate comparability of the results with other studies that may assess the upper cervical cord in different manners, e.g. using a different section length or other methods of cord area estimation, we also calculated the mean cross-sectional area within the selected section by dividing the volume by the defined section length (50 mm). Thus, when quantitative results are presented throughout this study, the mean cross-sectional area of the spinal cord section is shown. To correct for intra-individual variations due to gender, natural aging, body and head size, all spinal cord results were normalized by multiplying by the ratio of the mean intracranial

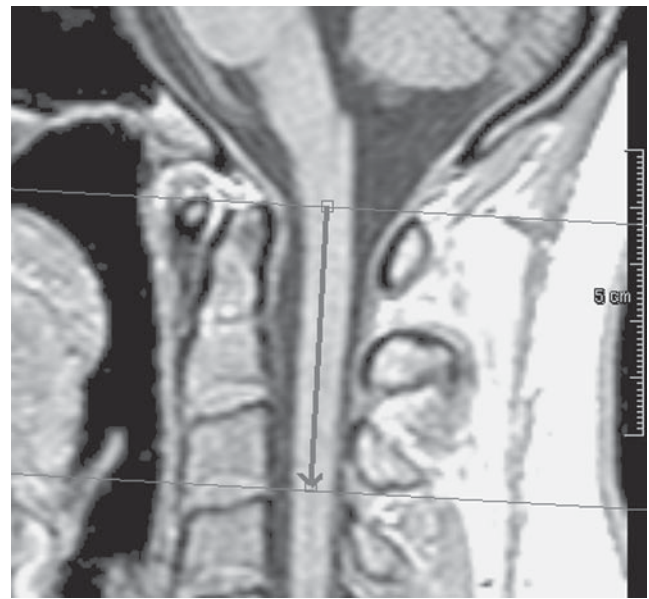


Fig. 1 Image post-processing by defining a volume of interest (VOI) starting at the upper borders of C2. The distance between both lines was set to a defined value of 50 mm

Table 1 Demographic data of SCA3 and SCA6 patients and healthy controls

	SCA3 (n = 14)	Healthy Controls (n = 14)	SCA6 (n = 10)	Healthy Controls (n = 10)
Sex (Male:Female)	10:4	10:4	7:3	7:3
Age (years), mean (range)	48 (27–67)	47 (33–69)	68 (59–75)	68 (58–76)
Mean age at disease onset (years)	41	–	59	–
ICARS, mean ± SD	33 ± 12	–	33.1 ± 15	–
Mean duration of disease (years)	6.9	–	9	–
CAG repeat length, mean (range)	69 (58–73)	–	22 (21–23)	–

cavity volume (ICC) of the total population to the ICC for each individual. The intracranial volume was assessed on the basis of the volumetric T1-weighted 3D data by using a semi-automated volumetry method for brain volumetry which is similar to the method used in [8] and described in more detail in [4]. In a preceding study on 40 healthy controls aged 24–76 years (data not published), we have shown that this normalization procedure corrects for the small age dependent decrease (<0.1% per year) in the mean cross-sectional area of the upper spinal cord and that this procedure reduces inter-individual variability of the mean cross-sectional area of the spinal cord (unpublished data).

■ Reproducibility

Intrarater reproducibility, interrater reproducibility and scan-rescan reproducibility of upper spinal cord volumetry were evaluated in a group of 18 healthy control subjects (10 female: age 24–59 years, mean 37 years; 8 male: age 25–57 years, mean 35 years) by two observers (C.L., B.B).

To evaluate the intrarater reproducibility, one investigator who was blinded to subjects' identity repeated the measurement at least one week apart. Similarly, interrater reproducibility was assessed by two independent investigators. Differences in paired data were analyzed and inter- and intrarater reproducibility for the group of subjects were expressed as the coefficient of variation (CV). The CV was calculated as the mean of the absolute differences of the data pairs divided by the mean of all volumetric values. Scan-rescan reproducibility was investigated in a subgroup of 5 subjects, who underwent serial MR imaging 3 to 5 times, resulting in 20 data pairs. To provide realistic conditions for serial imaging the subjects were either examined on different visits within one week, or completely repositioned between subsequent MR examinations. Scan-rescan reproducibility for this group of subjects was also expressed as CV. To facilitate comparability with other studies, mean cross-sectional area was calculated by dividing the volume by the defined section length (50 mm). Table 2 summarizes CVs and presents the group means for cross-sectional area.

■ Statistical analysis

Statistical analyses were performed using SPSS11 (SPSS Inc., Chicago, IL). Statistical comparison of the groups was performed by the Mann-Whitney U test. In case of multiple comparisons we corrected the p-values of the Mann-Whitney U test according to the Sidak stepdown procedure. In the Results section the adjusted p values are given.

To examine the effects of disease duration, CAG repeat length and ICARS on the normalized mean cross-sectional cord area in the SCA subtypes a multivariate regression analysis was performed.

Results

■ Reproducibility

The assessment of the intrarater variability revealed high reproducibility of mean cross-sectional area deter-

mination within the group of healthy control subjects with a CV below 0.6% for the upper cervical spinal cord. Interrater evaluation of the same datasets by two investigators gave a slightly higher CV value of 1.0%. The scan-rescan CV of 1.28% reflects high reproducibility of the quantification method (Table 2).

■ Quantification of spinal cord atrophy

A significant group difference in normalized mean cross-sectional area between the SCA3 group and controls ($p < 0.0005$) was found (Table 3). There was also a significant difference between the group mean values of both patient groups, showing lower values in the SCA3 group compared to SCA6 subjects ($p = 0.001$) (Fig. 2). Fig. 3 illustrates typical MRI findings in SCA3 and SCA6. In the SCA6 group, no group mean difference of the mean spinal cord area compared to healthy controls was found ($p = 0.379$) (Table 3). Neither in SCA3 ($p = 0.145$) nor in SCA6 ($p = 0.527$) was a dependency of mean cross-sectional areas on disease duration found (Table 4). In SCA3 we found a tendency to smaller cervical cord areas in more severely impaired patients (Fig. 4) but this did not reach significance ($p = 0.127$). SCA6 patients showed a negative dependency between the ICARS and spinal cord mean cross-sectional area with smaller cross-section areas in more severely impaired patients (Fig. 4; $p = 0.02$). No dependency was found for CAG repeat length and mean cross-sectional areas in both SCA subtypes (Table 4).

Exclusion of dysarthria and oculomotor subscores as pure cerebellar items did not increase the correlation of ICARS and mean normalized cross-sectional area in SCA6 ($p = 0.024$). In the SCA3 group, correlation of ICARS and mean normalized cross-sectional area improved after exclusion of pure cerebellar items, however still lacked significance ($p = 0.063$). When subdividing patients regarding clinical signs of pyramidal or sensory

Table 3 Mean cross-sectional area in SCA subtypes and controls

Type	Mean cross-sectional area (mm ²)	p-value
SCA3	59.02 ± 8.5	< 0.0005
Control group	82.17 ± 8.4	
SCA6	84.89 ± 9.8	0.379
Control group	82.39 ± 12.7	

Table 2 Intrarater, interrater and scan-rescan coefficients of variation and group mean cross-sectional area results

	Intrarater reproducibility	Interrater reproducibility	Scan-rescan reproducibility
CV ¹	0.57%	1.0%	1.28%
mean USC ² cross-sectional area	78.6 mm ²	78.6 mm ²	80.6 mm ²

¹ CV coefficient of variation; ² USC upper spinal cord

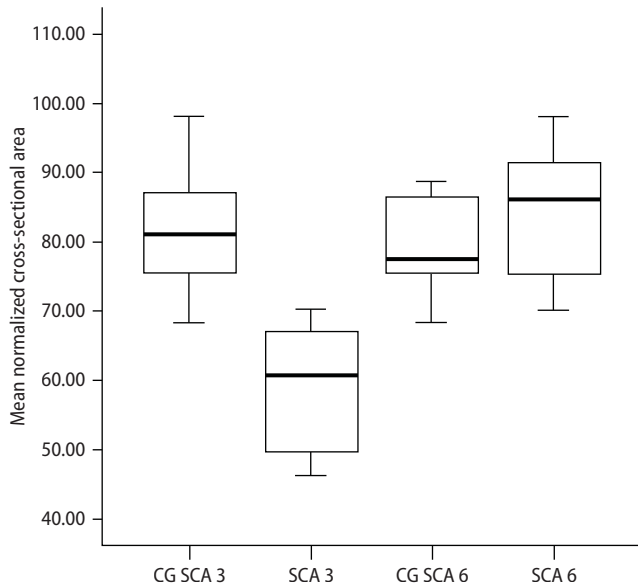


Fig. 2 Box plot of mean normalized upper cervical cord cross-sectional area in mm² from SCA3, SCA6 and corresponding control groups (CG). Box plot depicts the data ranges between the 25th and 75th percentile. The error bars give the data minimum and maximum

tract affection, the resulting subgroups were too small to permit any sensible analysis with one exception. Extensor plantar response in SCA3 was present in 6 of 14 patients and was correlated with smaller normalized cross-section areas in SCA3 patients ($p=0.043$).

All data are presented after normalization for head size. This procedure reduces the interindividual variability in healthy control individuals (Mean cross-sectional area in raw data: $78.6 \pm 7.7 \text{ mm}^2$ versus normalized data: $79.4 \pm 6.6 \text{ mm}^2$) and compensates for a small negative correlation between the uncorrected mean cross-sectional area and age within the healthy control group (Pearson's correlation analysis without normalization: $r = -0.307$, $p = 0.105$; after normalization: $r =$

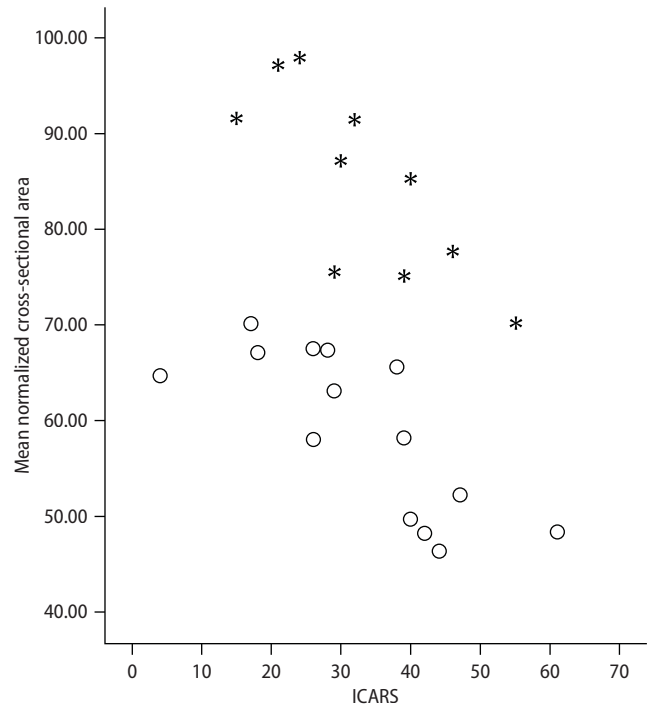
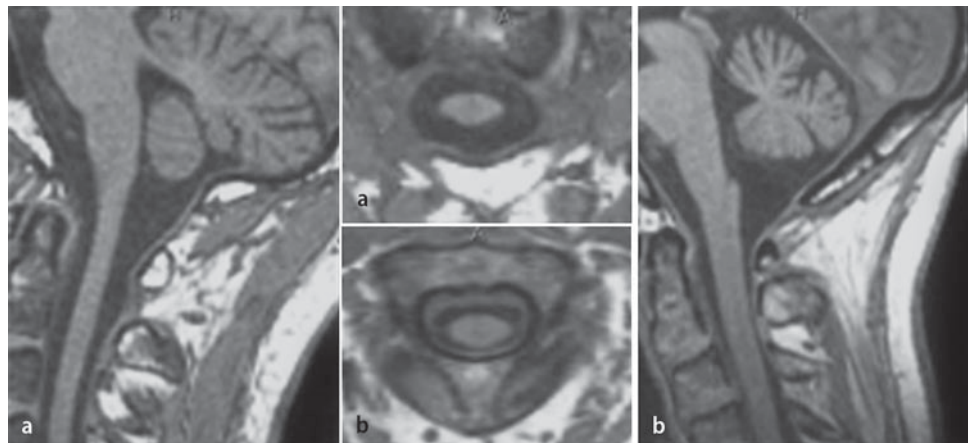


Fig. 4 Scatter plot of the mean normalized upper cervical cord cross-sectional area in mm² and ICARS from SCA3 (circles) and SCA6 (asterisks) patients

Table 4 Regression of CAG repeat length, disease duration and ICARS on mean cross-sectional area for SCA subtypes

Type	R ²	Independent variable	Regression coefficient	Standard error	p-value
SCA 3	0.672	CAG	-0.089	0.509	0.865
		Disease duration	-0.642	0.407	0.145
		ICARS	-0.287	0.173	0.127
SCA 6	0.655	CAG	-2.728	3.648	0.483
		Disease duration	-0.257	0.383	0.527
		ICARS	-0.636	0.204	0.021

Fig. 3 Sagittal and transversal T1-weighted images of the USC of typical SCA3 and SCA6 patients (**a**: SCA3 patient 54 y, m, disease duration 5 years, mean SCA area: 58 mm²; **b**: SCA6 patient 59 y, m, disease duration 4 years, mean USC area: 90 mm²). Beside cerebellar and brain stem atrophy, spinal cord atrophy is clearly visible in the SCA3 patient



-0.132, $p=0.495$). The normalization process did not change the significance of results compared to raw data analysis.

Discussion

In this first quantitative study of spinal cord atrophy in SCA, we observed characteristic genotype-specific differences of mean cross-sectional areas between SCA3 and SCA6. SCA3 patients had pronounced atrophy of the spinal cord even in mildly affected patients. Taking the short disease duration in the SCA3 group into account, upper spinal cord atrophy seems to be a phenomenon that may occur in SCA3 already in early and even presymptomatic phases of the disease. However, this has to be analyzed in prospective studies in SCA3. In contrast, SCA6 patients show no reduction of mean cross-sectional area in comparison to the control group. Our results are in accordance with pathoanatomic studies that found pure cerebellar degeneration in SCA6, whereas in SCA3 multiple additional parts of the nervous system, including basal ganglia, pontine nuclei and upper spinal cord were atrophic. Especially, anterior horn cells, Clark's columns, intermediolateral and dorsal columns and spinocerebellar tracts were shown to be affected in SCA3 [3, 11, 18, 19].

With regard to clinical disability, spinal cord area was smaller in more severely impaired patients (Fig. 4). The correlation may have missed significance in SCA3 because of small number of patients and, on the other hand, because of rather severe atrophy already in the early stages of the disease in patients with ICARS sum scores of 20 points or less. However, the presence of extensor plantar response in SCA3 was correlated with smaller spinal cord area. Prospective studies with repetitive MRI assessment will help to provide further

evidence to prove the functional relevance of spinal cord volume when worsening of ICARS values accompanies progression of cervical cord atrophy.

Although mean spinal cord area in the SCA6 group was not reduced compared to controls, lower mean cross-sectional areas correlated with clinical disability measured by ICARS. The functional relevance remains unclear. The normal spinal volume in the SCA6 group is in good agreement with the lack of gross changes of the spinal cord in post mortem analyses. However, increasing evidence points to additional involvement of brainstem and long fiber tracts in SCA6 that may have been missed so far since it is more subtle than in SCA3 (Udo Rüb, personal communication).

The procedure of MR volumetry used in this study has been evaluated as a fast and highly reliable technique for the assessment of upper cervical cord morphometry in vivo. This is a time-saving method, since average post-processing time of a complete 3D MRI dataset was only 5–10 minutes. Its functional relevance has been shown in patients with multiple sclerosis where the upper cervical cord area correlates with disability and is established as a biomarker of disease progression [7]. In SCA, prospective longitudinal studies are presently performed to assess progression of disability in the natural course of the disease [16]. Correlation of natural history data to serial MR volumetric measurements of the spinal cord will evaluate the upper cervical cord area as a biomarker for intervention studies in SCA3. Additionally, spinal cord volumetry should be investigated in other SCA genotypes like SCA1, SCA2 and SCA7 where post mortem studies suggested affection of the spinal cord similar to SCA3.

■ **Acknowledgement** The authors wish to thank S. Lange for helpful comments and statistical analysis. This study was supported partially by a grant from the Deutsche Forschungsgemeinschaft (SCHO 754/3-1) to LS.

References

1. Bakshi R, Dandamudi VS, Neema M, De C, Bermel RA (2005) Measurement of brain and spinal cord atrophy by magnetic resonance imaging as a tool to monitor multiple sclerosis. *J Neuroimaging* 15:30S–45S
2. De Michele G, Di Salle F, Filla A, D'Alessio G, Ambrosio G, Viscardi L, Scala R, Campanella G (1995) Magnetic resonance imaging in "typical" and "late onset" Friedreich's disease and early onset cerebellar ataxia with retained tendon reflexes. *Ital J Neurol Sci* 16:303–308
3. Dürr A, Stevanin G, Cancel G, Duyckaerts C, Abbas N, Didierjean O, Chneiweiss H, Benomar A, Lyon-Caen O, Julien J, Serdaru M, Penet C, Agid Y, Brice A (1996) Spinocerebellar ataxia 3 and Machado-Joseph disease: clinical, molecular, and neuropathological features. *Ann Neurol* 39:490–499
4. Hahn HK, Millar WS, Klinghammer O, Durkin MS, Tulipano PK, Peitgen HO (2004) A Reliable and Efficient Method for Cerebral Ventricular Volumetry in Pediatric Neuroimaging. *Methods Inf Med* 43(4):376–382
5. Klockgether T, Ludtke R, Kramer B, Abele M, Bürk K, Schöls L, Riess O, Laccone F, Boesch S, Lopes-Cendes I, Brice A, Inzelberg R, Zilber N, Dichgans J (1998) The natural history of degenerative ataxia: a retrospective study in 466 patients. *Brain* 121: 589–600
6. Klockgether T, Skalej M, Wedekind D, Luft AR, Welte D, Schulz JB, Abele M, Bürk K, Laccone F, Brice A, Dichgans J (1998) Autosomal dominant cerebellar ataxia type I. MRI-based volumetry of posterior fossa structures and basal ganglia in spinocerebellar ataxia types 1, 2 and 3. *Brain* 121:1687–1693

7. Lukas C, Bellenberg B, Rexilius J, Hahn HK, Kahle M, Köster O, Schimrigk SK (2006) MR-based measurement of spinal cord atrophy in multiple sclerosis: Reproducibility and sensitivity of a new semi-automated procedure. *Eur Radiol* 16:458
8. Lukas C, Hahn HK, Bellenberg B, Rexilius J, Schmid G, Schimrigk SK, Przuntek H, Köster O, Peitgen HO (2004) Sensitivity and reproducibility of a new fast 3D segmentation technique for clinical MR-based brain volumetry in multiple sclerosis. *Neuroradiology* 46:906–915
9. Mascalchi M, Salvi F, Piacentini S, Bartolozzi C (1994) Friedreich's ataxia: MR findings involving the cervical portion of the spinal cord. *AJR Am J Roentgenol* 163:187–191
10. Miller DH (2004) Biomarkers and surrogate outcomes in neurodegenerative disease: lessons from multiple sclerosis. *NeuroRx* 1:284–294
11. Munoz E, Rey MJ, Mila M, Cardozo A, Ribalta T, Tolosa E, Ferrer I (2002) Intracellular inclusions, neuronal loss and CAG mosaicism in two patients with Machado-Joseph disease. *J Neurol Sci* 200:19–25
12. Murata Y, Kawakami H, Yamaguchi S, Nishimura M, Kohriyama T, Ishizaki F, Matsuyama Z, Mimori Y, Nakamura S (1998) Characteristic magnetic resonance imaging findings in spinocerebellar ataxia 6. *Arch Neurol* 55:1348–1352
13. Murata Y, Yamaguchi S, Kawakami H, Imon Y, Maruyama H, Sakai T, Kazuta T, Ohtake T, Nishimura M, Saida T, Chiba S, Oh-i T, Nakamura S (1998) Characteristic magnetic resonance imaging findings in Machado-Joseph disease. *Arch Neurol* 55:33–37
14. Rashid W, Davies GR, Chard DT, Griffin CM, Altmann DR, Gordon R, Thompson AJ, Miller DH (2006) Increasing cord atrophy in early relapsing-remitting multiple sclerosis: a 3 year study. *J Neurol Neurosurg Psychiatry* 77:51–55
15. Satoh JI, Tokumoto H, Yukitake M, Matsui M, Matsuyama Z, Kawakami H, Nakamura S, Kuroda Y (1998) Spinocerebellar ataxia type 6: MRI of three Japanese patients. *Neuroradiology* 40:222–227
16. Schmitz-Hübsch T, du Montcel ST, Baliko L, Berciano J, Boesch S, Depondt C, Giunti P, Globas C, Infante J, Kang JS, Kremer B, Mariotti C, Melegh B, Pandolfo M, Rakowicz M, Ribai P, Rola R, Schols L, Szymanski S, van de Warrenburg BP, Dürr A, Klockgether T (2006) Scale for the assessment and rating of ataxia: development of a new clinical scale. *Neurology* 66:1717–1720
17. Schöls L, Amoiridis G, Büttner T, Przuntek H, Epplen JT, Riess O (1997) Autosomal dominant cerebellar ataxia: phenotypic differences in genetically defined subtypes? *Ann Neurol* 42:924–932
18. Schöls L, Bauer P, Schmidt T, Schulte T, Riess O (2004) Autosomal dominant cerebellar ataxias: clinical features, genetics, and pathogenesis. *Lancet Neurol* 3:291–304
19. Takiyama Y, Oyanagi S, Kawashima S, Sakamoto H, Saito K, Yoshida M, Tsuji S, Mizuno Y, Nishizawa M (1994) A clinical and pathologic study of a large Japanese family with Machado-Joseph disease tightly linked to the DNA markers on chromosome 14q. *Neurology* 44:1302–1308
20. Trouillas P, Takayanagi T, Hallett M, Currier RD, Subramony SH, Wessel K, Bryer A, Diener HC, Massaquoi S, Gomez CM, Coutinho P, Ben Hamida M, Campanella G, Filla A, Schut L, Timann D, Honnorat J, Nighoghossian N, Manyam B (1997) International Cooperative Ataxia Rating Scale for pharmacological assessment of the cerebellar syndrome. The Ataxia Neuropharmacology Committee of the World Federation of Neurology. *J Neurol Sci* 145:205–211
21. Villanueva-Haba V, Garcés-Sánchez M, Bataller L, Palau F, Vilchez J (2001) Neuroimaging study with morphometric analysis of hereditary and idiopathic ataxia. *Neurologia* 16:105–111
22. Wessel K, Schroth G, Diener HC, Müller-Forell W, Dichgans J (1989) Significance of MRI-confirmed atrophy of the cranial spinal cord in Friedreich's ataxia. *Eur Arch Psychiatry Neurol Sci* 238:225–230
23. Yoshizawa T, Watanabe M, Frusho K, Shoji S (2003) Magnetic resonance imaging demonstrates differential atrophy of pontine base and tegmentum in Machado-Joseph disease. *J Neurol Sci* 215:45–50